Reduction of external quantum efficiency of ultraviolet LEDs caused by overdoping of barriers with silicon

© E.I. Shabunina[1], N.M. Shmidt[1], A.E. Chernyakov[2], N.A. Talnishnikh[2], A.L. Zakgeim[2], A.E. Ivanov[2,3], L.A. Aleksanyan[4], A.Ya. Polyakov[4]

[1] Ioffe Institute,
194021 St. Petersburg, Russia
[2] SHM R&E Center, Russian Academy of Sciences,
194021 St. Petersburg, Russia
[3] St. Petersburg Electrotechnical University „LETI“,
197022 St. Petersburg, Russia
[4] National University of Science and Technology „MISIS“,
119049 Moscow, Russia

E-mail: jenni-85@mail.ru

Received May 5, 2025
Revised June 24, 2025
Accepted September 18, 2025

Commercial AlGaN ultraviolet (UV) LEDs with emission wavelength of 270−280 nm and external quantum efficiency (EQE) of 5−7% were studied. $C-V$ profiling revealed an order of magnitude higher electron concentration in the active region compared to blue LEDs, caused by overdoping with silicon. Analysis of electroluminescence spectra and frequency dependences of the spectral density of low-frequency noise revealed the rearrangement of excited defects in UV LEDs at injection levels an order of magnitude lower than in blue LEDs, as well as the onset of defect generation during aging after 25 hours.

Keywords: LEDs, UV range, MQW, AlGaN/GaN, low-frequency noise.

DOI: 10.61011/SC.2025.07.62470.8101

Ultraviolet-range (UV) LEDs based on quantum-dimensional AlGaN/GaN structures, emitting at a wavelength of 280 nm and shorter, are of interest for use in disinfection of water purification, in satellite communications [1–3]. However, the potential of these LEDs has not been realized so far. Low values of external quantum efficiency (EQE) and service life, which are several times lower than the EQE of blue InGaN/GaN LEDs, are the main obstacle [4,5]. A large number of studies [6,7] is devoted to elucidating the factors leading to such a gap between the parameters of UV and blue LEDs based on nitrides. Among such factors . low internal efficiency [2], caused by the worst ordering of the AlGaN nanomaterial with a high aluminum content. As a result, the blurring of the heterogeneous boundaries increases [8,9], as well as the concentration of local regions with a nonequilibrium composition of the solid solution and excited defects [8]. In addition, hole injection worsens with an increase in the activation energy of magnesium with an increase in the aluminum content [2]. An additional factor is the problems with the output of radiation [1,2]. Judging by the features of the current–voltage characteristic of UV LEDs, the tunneling component of the direct branch current contributes to significantly higher bias voltages than in blue LEDs, which can be caused by tunneling of charge carriers both in random fluctuations in composition and due to the high concentration of charge carriers in the active region of the LED.

In this paper, the charge carrier distribution profiles in the active regions of UV, blue, and green LEDs are investigated and the possible effect of the concentration of electrons and silicon in the active region and related phenomena on the reduction of EQE and the service life of UV LEDs is clarified.

Commercial AlGaN UV LEDs 4550-Mil-Bare Chip (Bolb Inc. USA) with a radiation wavelength of 270−280 nm, grown by MOCVD on AlN/sapphire substrates are studied in this paper. The active region contains AlGaN quantum wells (QWs). The area of the active region is 1.4 mm^2, radiation output was carried out through a substrate, flip-chip mounting with a radiator. The maximum values of EQE are 7%. Current–voltage characteristic (I-V), capacitance dependences on applied voltage ($C-V$), electroluminescence spectra (EL) and frequency dependences of the spectral density of low-frequency current noise (S_I) in the frequency range of 1−1000 Hz were measured. The I-V was measured using the KEITHLEY 6487 system. The EL spectra were measured in the integration area of the OL770-LEDUF-/VIS High-speed LED Test and Measurement System (Optronic Laboratories Inc., USA) with a high-speed THORLABS DET02AFC/M photodetector. The frequency dependences S_I of LEDs were measured in a circuit with a SR560 preamplifier (Stanford Research Systems, Sunnyvale, USA) and a SR 770 FET NETWORK Analyzer (Stanford Research Systems, Sunnyvale, USA). The level of low-frequency noise and the features of the type of frequency dependence of low-frequency current noise S_I carry integral information about defects, and the slope of the dependence $S_I \sim 1/f^{\nu}$, where ν is an indicator of the

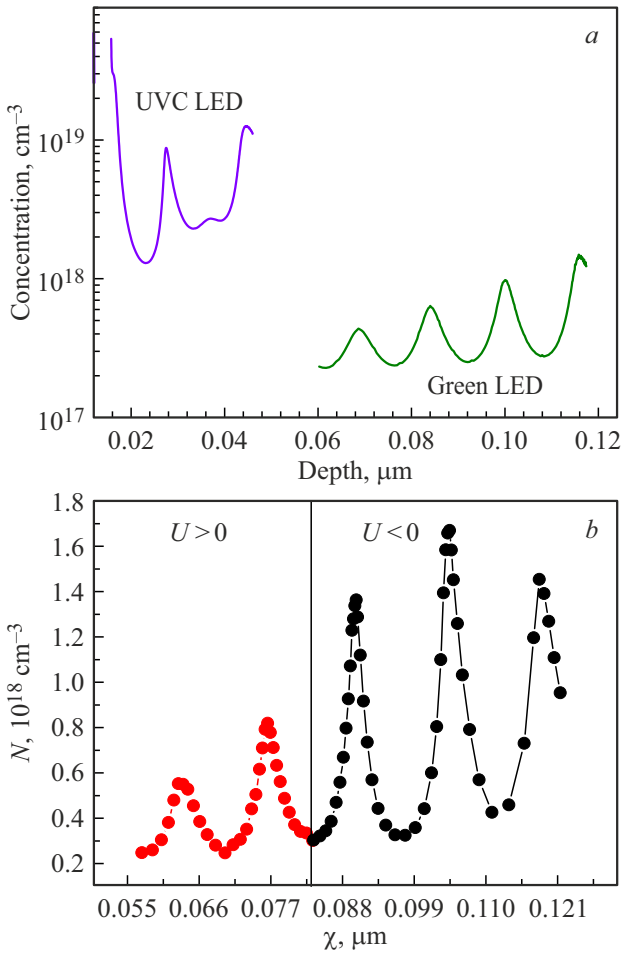

Figure 1. Charge carrier distribution profiles in UV and green LEDs (a) and in blue LEDs in the voltage range (U) from +1.5 to −3 V (b).

shape of the spectrum, allows tracing the evolution of the magnitude of micro-stresses in the LED with a change of $\nu > 1$. The change in this parameter at $\nu < 1$ in the range of $f > 100$ Hz reflects the contribution to low-frequency noise caused by generation-recombination processes on Shockley-Reed-Hall defects [10]. The aging tests of the LEDs were carried out at a direct current of 350 mA in the forward direction at a temperature of 20 °C.

Measurements of $C-V$-dependences in the voltage range (U) from +1.5 to −3 V allow calculating the distribution profile of charge carriers over the depth of the active region of LEDs (Figure 1, a and b) according to the known ratios [11]. It is clearly seen that the concentration of charge carriers in the UV LED (Figure 1, a) is an order of magnitude higher, both in wells and in barriers, than the concentration in green (Figure 1, a) and blue (Figure 1, b) LEDs. The fact is that, starting with the paper of Yunovich et al. [12], which revealed the presence of charged acceptor-type defects in the active region of LEDs, doping of the active region with silicon was introduced into LED technology to compensate for charged centers. This operation made it possible to increase the EQE of the LEDs. However, it turned out that the more disordered the nanomaterial is, the higher the level of silicon doping [13]. An analysis of studies of the morphology of AlGaN/GaN structures with a high aluminum content shows that the ordering of the nanomaterial of these structures is inferior to the ordering of InGaN/GaN LEDs, especially blue ones with a lower indium content. This is why the active region of UV LEDs is redoped with silicon. Silicon not only supplies electrons, but it can also change the symmetry of the lattice, since the tetrahedral radius of silicon is smaller than that of gallium, but larger than that of nitrogen. These changes can increase the concentration of excited defects having excessive elastic energy. According to the theoretical concepts of the properties of such centers [14], they should complicate the processes of recombination and change their properties with increasing concentration of charge carriers.

Study of the dependence of the spectral density of low-frequency current noise (S_I) on frequency, in the range of 1–1000 Hz, commercial UV LEDs at a wavelength of 280 nm with EQE of 5–7% revealed the presence of such centers, which are not observed in blue and green LEDs at low injection levels. The change of the type of dependence $S_I(f)$ is observed for all UV LEDs starting from low current values of 10^{-5} A. The slope of S_I (f) changes from $S_I \sim 1/f$ to $S_I \sim 1/f^{\nu}$, where ν is an indicator of the shape of the spectrum > 1 at frequencies of < 100 Hz (Figure 2, a and b). According to theoretical concepts, this type of dependence indicates mechanical microstress in the active region of LEDs [10]. At the same time, a decrease in the value of ν is observed with an increase in the injection current from $5 \cdot 10^{-5}$ A to 1.5 mA, i. e., the level of mechanical stresses decreases. There are two typical variations in the value of ν, shown in Figure 2, a LEDs B9 and B10 (Figure 2, b). The features of the defective structure are manifested in these LEDs at a minimum current of $5 \cdot 10^{-5}$ A. A slight increase of $\nu = 1.1$ is observed at frequencies of < 100 Hz for the B9 LED, which indicates an increase of microstresses. At the same time, a slope of dependence $\nu = 0.8$ is observed in the frequency range of > 100 Hz. According to theoretical concepts, a superposition of the dependence $1/f$ and the generation-recombination component associated with the presence of single Shockley-Reed-Hall defects is observed in this frequency range. As the current increases, the microstresses increase slightly, ν increases to 1.2, and the contribution of the generation-recombination component increases. For the B10 LED at minimum currents, the dependence is determined by noise $1/f$, i. e., closely spaced defects in the entire frequency range, and the level of this noise is higher than that of the B9 LED. It should be noted that the concentration of charge carriers in the LED B10 is 1.5 times higher than concentration of charge carriers in B9, however, this difference is insignificant against the background of the values of 10^{19} cm $^{-3}$. The changes in microstress are more significant. As the current increases, the microstresseses increase, and they are higher than microstresseses of B9,

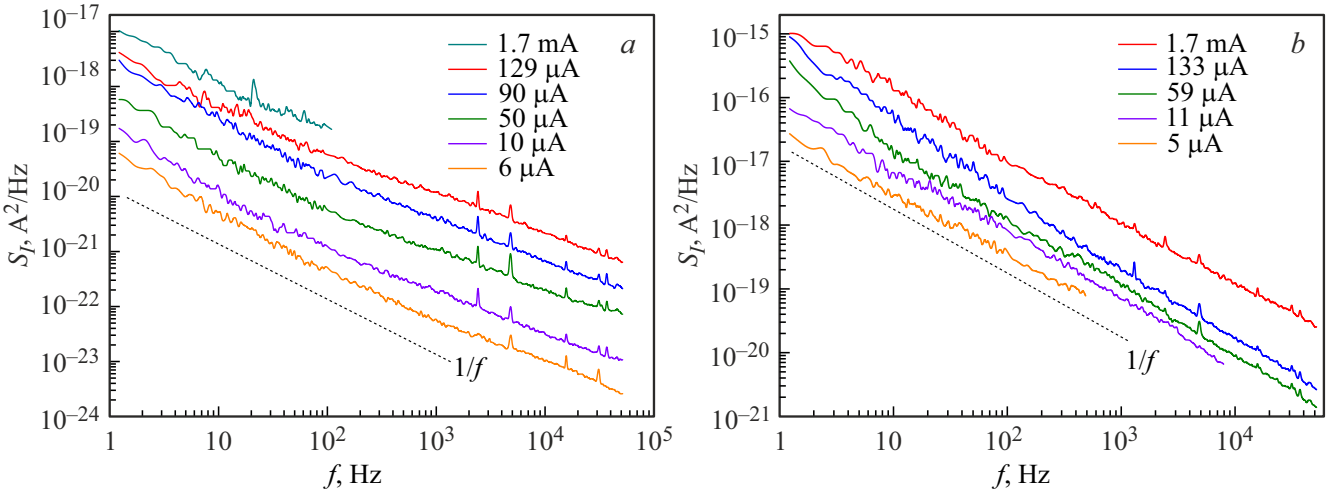

Figure 2. Frequency dependences of the spectral density of low-frequency current noise of two UV LEDs: B9 (*a*) and B10 (*b*).

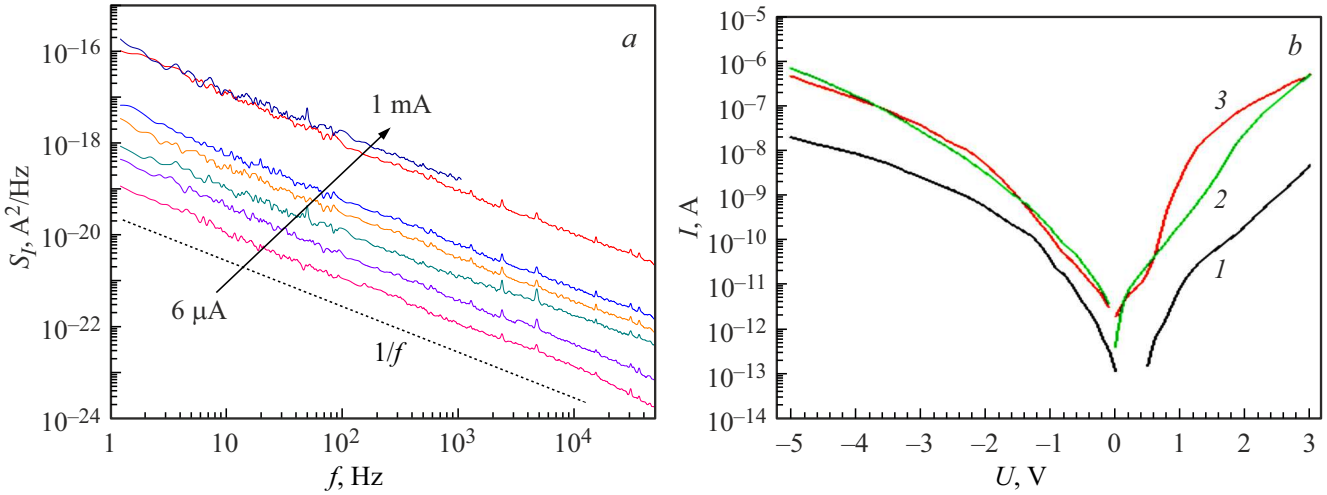

Figure 3. *a* — frequency dependence of the spectral density of current noise of a blue LED. *b* — evolution of VAX during aging of UV LEDs B9 and B10: *1* — initial I-V, *2* — restored I-V B9 after 75 h aging and B10 after 50 h, *3* — I-V B9 — after 50 h and B10 after 25 h.

$\nu = 1.3$ at frequencies of < 100 Hz, and the contribution of the generation-recombination component appears only at a current of 1.7 mA, and it is less, since $\nu = 0.9$. For efficient blue and green LEDs with maximum EQE values at such low tuning currents, there are no defects in the system and frequency dependencies over the entire frequency range reveal the presence of closely spaced centers and the absence of microstress (Figure 3, *a*). The results obtained suggest that the rearrangement of the active region by silicon leads to a greater symmetry violation in the lattice and a higher concentration of excited defects than in blue and green LEDs, as well as to the generation of Shockley-Reed-Hall defects. In addition, the electron concentration in the active region is significantly higher in UV LEDs. As a result, coordination rearrangement begins at low injection levels. Experiments on the aging of these two types of LEDs with different features have shown that for the B10 LED, changes in the defective system begin after 25 hours of operation at room temperature at operating current, which is revealed by a change in I-V (Figure 3, *b*, curve *3*). For the B9 LED, the same changes are observed only after 50 hours of aging. Current–voltage characteristic of B9 and B10, i. e. the initial I-V and I-V after 50 and 25 h, respectively, practically coincide, therefore one curve is given for each case. After an additional 25 h of aging, a partial recovery of the I-V is observed (Figure 3, *b*, curve *2*). The current–voltage characteristic of B9 and B10 after 50 and 25 hours, respectively, are almost the same, so one curve is shown. As it was shown earlier, this behavior during aging [8] is caused by the peculiarities of the interaction of excited defects with charge carriers, which cause a coordination rearrangement of excited defects. The level of low-frequency noise in UV LEDs is an order of magnitude higher, indicating a higher concentration of defects. The radiative

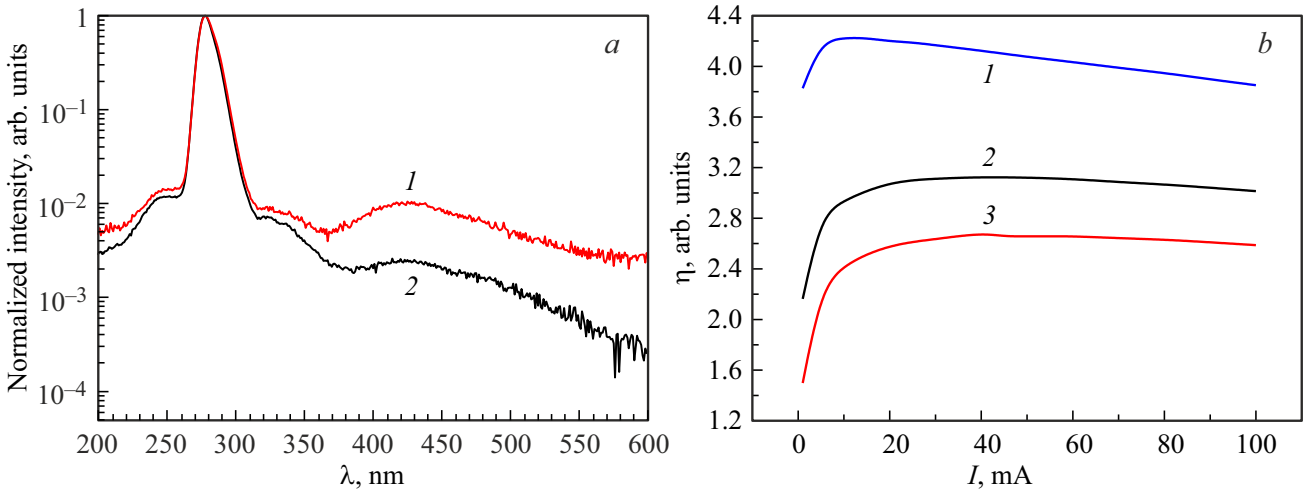

Figure 4. *a* — electroluminescence spectrum of a UV LED at currents, mA: *1* — 1, *2* — 300. *b* — efficiency dependences in relative units of a UV LED from current at temperatures, K: *1* — 223, *2* — 293, *3* — 323.

recombination is observed at a current of 1 mA in the LED electroluminescence spectra (Figure 4, *a*, curve *1*), but not only in the maximum at a wavelength of 280 nm, but also in the defective band of 350–560 nm, as well as in areas with a different composition of the solid solution. At low excitation levels, charge carriers are lost to radiative recombination in defective regions of the solid solution and in GaN barriers. In addition, the loss of charge carriers is caused by recombination on excited defects and their rearrangement. As the temperature drops to 223 K, the carrier concentration in the active region decreases, and the EQE at its maximum increases by 30% (Figure 4, *b*, curve *1*) relative to the efficiency at 293 K (Figure 4, *b*, curve *2*). The results obtained suggest that the rearrangement of the active region of UV LEDs introduces additional excited and Shockley-Reed-Hall defects and reduces the values of the EQE to a maximum, as well as accelerates the generation of defects during aging. Thus, the rearrangement of the active region by silicon increases the loss of charge carriers caused by the decomposition of the solid solution. It seems that reducing the level of silicon doping by several times and preventing the decomposition of the solid solution will increase the quantum efficiency and service life of UV LEDs.

Conflict of interest

The authors declare that they have no conflict of interest.

References

[1] H. Xu, H. Long,, J. Jiang, M. Sheikhi, L. Li, W. Guo, J. Dai, C. Chen, J. Ye. Nanotechnology, **30**, 435202 (2019). DOI: 10.1088/1361-6528/ab3208
[2] M. Kneissl, T.Y. Seong, H. Jung, A. Hiroshi. Nat. Photonics, **13**, 233 (2019).
[3] Q. Ong, J.W.R. Teo, J.D. Cruz, E. Wee, W. Wee, W. Han. Heliyon, **8**, 11132 (2022). https://doi.org/10.1016/j.heliyon.2022.e11132
[4] M. Su, H. Liu, M. Cai, W. Sun. IEEE Trans. Electron Dev., **70** (2), 570 (2023).
[5] F. Piva, M. Buffolo, N. Roccato, M. Pilati, S. Longato, N. Susilo, D.H. Vidal, A. Muhin, L. Sulmoni, T. Wernicke, M. Kneissl, C.D. Santi, G. Meneghesso, E. Zanoni, M. Meneghini. Semicond. Sci. Technol., **39**, 075025 (2024). https://doi.org/10.1088/1361-6641/ad54e9
[6] H. Hirayama, T. Takano, M.S. Jun, T. Takuya, M. Kenji, J. Noritoshi, I.O. Masafumi, M. Issei, K. Takuma. Proc. SPIE, **10104**, 101041 (2017).
[7] M. Su, H. Liu, M. Cai, W. Sun. IEEE Trans. Electron Dev., **70** (2), 570 (2023).
[8] G. Savchenko, E. Shabunina, A. Chernyakov, N. Talnishnikh, A. Ivanov, A. Abramov, A. Zakgeim, V. Kuchinskii, G. Sokolovskii, N. Averkiev, N. Shmidt. Nanomaterials, **14**, 1072 (2024). https://doi.org/10.3390/
[9] V. Davydov, E.M. Roginskii, Y. Kitaev, A. Smirnov, I. Eliseyev, E. Zavarin, W. Lundin, D. Nechaev, V. Jmerik, M. Smirnov, M. Pristovsek, T. Shubina. Nanomaterials, **11**, 2396 (2021). https://doi.org/10.3390/nano11092396
[10] G.P. Zhigal'skii. *Fluktuatsii i shumy v elektronnykh tverdotel'nykh priborakh* (Fizmatlit, M., 2012). (in Russian).
[11] S. Zi. *Fizika poluprovodnikovyk priborov* (M., Mir, 1984) ch. 1. (in Russian).
[12] S.S. Mamakin, A.E. Yunovich, A.B. Vattana, F.I. Manyakhin. FTP, **37**, 1131 (2003). (in Russian).
[13] V.M. Busov, V.V. Emtsev, R.N. Kyutt, V.V. Lundin, D.S. Poloskin, V.V. Ratnikov, A.V. Sakharov, N.M. Shmidt. Solid State Phenomena, **69-70**, 525 (1999).
[14] V.N. Abakumov, V.I. Perel, I.N. Yassievich, G.V. Gordeeva. *Nonradiative Recombination in Semiconductors; Modern Problems in Condensed Matter Sciences* (North-Holland, Amsterdam–Oxford–N.Y., 1991).

Translated by A.Akhtyamov